Available online at www.sciencedirect.com
SCIENCE DIRECT®
Journal of Power Sources 145 (2005) 10–15
JOURNAL OF POWER SOURCES
www.elsevier.com/locate/jpowsour

Short communication

Partial oxidation of ethanol on supported Pt catalysts

Lisiane V. Mattos, Fábio B. Noronha *

Instituto Nacional de Tecnologia (INT), Laboratório de Catálise, sala 518, Av. Venezuela 82, CEP 20081-312, Rio de Janeiro, Brazil

Received 25 November 2004; accepted 19 December 2004
Available online 17 February 2005

Abstract

This work studied the effect of the nature of the support on the performance of Pt/Al_2O_3, Pt/ZrO_2, Pt/CeO_2 and $Pt/Ce_{0.50}Zr_{0.50}O_2$ catalysts on partial oxidation of ethanol. The reducibility and oxygen transfer capacity were evaluated by temperature-programmed reduction (TPR) and oxygen storage capacity (OSC) experiments. The results showed that the support plays an important role on the products distribution of the partial oxidation of ethanol. Acetic acid was the main product on Pt/Al_2O_3 catalyst whereas methane and acetaldehyde were the only products detected on Pt/ZrO_2, Pt/CeO_2 and $Pt/Ce_{0.50}Zr_{0.50}O_2$ catalysts.

The products distribution obtained on Pt/ZrO_2, Pt/CeO_2 and $Pt/Ce_{0.50}Zr_{0.50}O_2$ catalysts was related to their redox properties. The OSC experiments showed that the oxygen exchange capacity was higher on Pt/CeO_2 and $Pt/Ce_{0.50}Zr_{0.50}O_2$ catalysts. A high oxygen storage capacity favored the formation of acetate species, which could be decomposed to CH_4 and/or oxidized to CO_2 via carbonate species. On the other hand, the lower oxygen exchange capacity of Pt/ZrO_2 catalyst led to a higher ethoxy species formation. These species can be dehydrogenated and desorb as acetaldehyde. Then, the higher selectivity to acetaldehyde observed on Pt/ZrO_2 catalyst could be assigned to its low oxygen storage/release capacity.

In the case of Pt/Al_2O_3 catalyst, the production of acetic acid could be related to its acidic properties, since this material did not show redox properties, as revealed by OSC analysis.

Keywords: Fuel cell; Partial oxidation of ethanol; Hydrogen production; Pt/Al_2O_3 catalyst; Pt/ZrO_2 catalyst; Pt/CeO_2 catalyst; $Pt/Ce_{0.50}Zr_{0.50}O_2$ catalyst

1. Introduction

Today, hydrogen is widely used as a feedstock in the petroleum (hydrocracking and hydrotreatment process), chemical (methanol and ammonia synthesis), food processing (oil and fat hydrogenation), steel and electronics industries [1,2]. However, hydrogen is not produced as an energy carrier or as a fuel for energy generation by the current industry.

The use of hydrogen as an energy carrier can support sustainable global economic growth as well as reduce the effects of air pollution and greenhouse gas emissions. But, there are several technological barriers that must be overcome to produce and deliver the large amounts of hydrogen that will be required in a hydrogen economy. One of the most significant barrier is the lack of existing infrastructure for both production and delivery of hydrogen [3]. In the absence of a hydrogen infrastructure, distributed production through small fuel processors at the refueling stations and at the stationary power generation plants is an attractive near- to mid-term approach for supplying hydrogen as an energy carrier.

Several technologies such as steam reforming, partial oxidation and autothermal reforming have been used to produce hydrogen from different feedstock (hydrocarbons like methane and gasoline, alcohols such as methanol and ethanol) [4].

In contrast to fossil fuel, ethanol is a renewable raw material that can be obtained from biomass and address the issue of the greenhouse effect. Furthermore, the infrastructure needed for ethanol production and distribution is already established in countries like Brazil and USA since ethanol is

* Corresponding author. Tel.: +55 21 2123 1177; fax: +55 21 2123 1051.
E-mail address: fabiobel@int.gov.br (F.B. Noronha).

0378-7753/$ – see front matter © 2005 Elsevier B.V. All rights reserved.
doi:10.1016/j.jpowsour.2004.12.034

currently distributed and used as an octane enhancer or oxygenate blended with gasoline. According to automobile manufacturers, fuel infrastructure is one of the most critical issues in determining the choice of fuel for fuel cell powered vehicles [5].

Steam reforming of ethanol has been proposed for the production of hydrogen to fuel cells [6–19]. However, this process presents some disadvantages such as formation of by-products and catalyst deactivation. Therefore, it is necessary to develop catalysts which are highly active, selective and stable under reaction conditions. Some authors have studied the effect of the support on performance of supported metallic catalysts on this reaction [16–19]. They concluded that the support plays a significant role on steam reforming of ethanol.

Coleman and co-workers [16] studied the behavior of alumina and ceria/zirconia-supported catalysts on steam reforming of ethanol. On alumina-supported catalysts, they observed that the ethene is the main product at lower temperatures. When the temperature is increased, the ethene is converted into H_2, CO, CO_2 and CH_4. For ceria/zirconia-supported catalysts, the formation of ethene is not observed. The main products obtained are H_2, CO, CO_2 and CH_4 even at lower temperatures.

Batista et al. [17] showed that the support affected the selectivity to products on steam reforming of ethanol over Co/Al_2O_3, Co/SiO_2 and CoMgO catalysts. According to these authors, hydrogen is the main product for all catalysts. The production of CO, CO_2, CH_4 and ethylene was also observed. Ethylene was only detected on Co/Al_2O_3. It was formed by dehydration of ethanol on acid sites of alumina. Co/SiO_2 exhibit the highest amount of methane, while Co/MgO showed the highest CO formation. All catalysts present a deactivation, which was more significant on a Co/Al_2O_3 catalyst. The deactivation was attributed to coke formation. In the case of Co/Al_2O_3, the acid sites of alumina promote carbon deposition. Llorca et al. [18] also studied steam reforming of ethanol on supported Co catalysts (Co/MgO, Co/Al_2O_3, Co/SiO_2, Co/TiO_2, Co/V_2O_5, Co/ZnO, Co/La_2O_3, Co/CeO_2 and Co/Sm_2O_3). They showed that Co/ZnO catalyst exhibit the higher H_2 and CO_2 production and no deactivation was observed on this catalyst during the reaction.

The effect of the support on the performance of supported Ni catalysts on steam reforming of ethanol was reported by Fatsikostas et al. [19]. The results showed that Ni/La_2O_3 catalyst presents the higher activity and selectivity towards H_2 than Ni/Al_2O_3, Ni/YSZ and Ni/MgO catalysts. The high stability of this catalyst was assigned to scavenging of coke deposition on the Ni surface by lanthanum oxycarbonate species which exist on top of the Ni particles during the reaction.

Although several authors have studied the performance of metal-based catalysts on steam reforming of ethanol, few works on the use of supported metallic catalysts on partial oxidation of ethanol are available in the literature [20–22].The partial oxidation reaction has fast start up and response time, which makes it a very interesting system. Furthermore, since this reaction does not need the indirect addition of heat via a heat exchanger, the POX reactor is more compact than a steam reformer.

We have previously reported that Pt/CeO_2 catalysts showed a good stability and high activity on partial oxidation of ethanol [20]. In order to explain the selectivities obtained on these catalysts, we proposed a reaction mechanism, using the IR, TPD and TPSR experiments. According to this mechanism, adsorption of ethanol on the support give rise to ethoxy species. A fraction of the ethoxy species can be dehydrogenated, which readily react with oxygen from the support producing acetate species and Ce^{3+}. Increasing the temperature, another fraction of the ethoxy species can be decomposed on Pt sites, forming CH_4, H_2 and CO while the acetate species previously formed can be decomposed to CH_4 and/or oxidized to CO_2 via carbonate species. Under oxygen atmosphere, the intermediate dehydrogenated species formed may desorb as acetaldehyde.

The goal of this work is to study the effect of the support on the performance of Pt based catalysts on partial oxidation of ethanol.

2. Experimental

2.1. Catalyst preparation

Al_2O_3, ZrO_2 and CeO_2 supports were prepared by calcination of γ-alumina (Engelhard Corporation Catalyst), zirconium hydroxide (MEL Chemicals) and cerium (IV) ammonium nitrate (Aldrich), respectively, at 1073 K, for 1 h, in a muffle. $Ce_{0.50}Zr_{0.50}O_2$ support was synthesized following the method published by Hori et al. [23]. An aqueous solution of cerium (IV) ammonium nitrate and zirconium nitrate (Aldrich) was prepared with 50 mol% CeO_2 and 50 mol% ZrO_2. Then, ceria and zirconium hydroxides were co-precipitated by the addition of an excess of ammonium hydroxide. Finally, the precipitate was washed with distillated water and calcined at 1073 K for 1 h in a muffle. Platinum (1.5 wt.%) was added to Al_2O_3, ZrO_2, CeO_2 and $Ce_{0.50}Zr_{0.50}O_2$ supports by incipient wetness impregnation with an aqueous solution containing $H_2PtCl_6{\cdot}6H_2O$ (Aldrich). After impregnation, the samples were dried at 393 K and calcined under air (50 $cm^3\,min^{-1}$) at 673 K, for 2 h. Then, four catalysts were obtained: Pt/Al_2O_3, Pt/ZrO_2, Pt/CeO_2 and $Pt/Ce_{0.50}Zr_{0.50}O_2$.

2.2. BET surface area

The BET surface areas of catalysts were measured using a Micromeritics ASAP 2000 analyzer by nitrogen adsorption at liquid nitrogen temperature.

2.3. X-ray diffraction (XRD)

X-ray diffraction measurements were carried out using a RIGAKU diffractometer with a Cu Kα radiation. After

calcination at 1073 K of supports, the XRD data were collected at 0.04° per step with integration times of 1 s per step.

2.4. Temperature-programmed reduction (TPR)

Temperature-programmed reduction (TPR) analyses were performed in a micro-reactor coupled to a quadrupole mass spectrometer (Balzers, Omnistar). The samples (300 mg) were dehydrated at 423 K, for 30 min, in a He flow prior to reduction. After cooling to room temperature, a mixture of 5% H_2 in Ar flowed through the sample at 30 $cm^3\ min^{-1}$, and the temperature was raised at a heating rate of 10 K min^{-1} up to 1273 K.

2.5. Oxygen storage capacity (OSC)

Oxygen storage capacity (OSC) measurements were carried out in the same apparatus previously described to TPR analyses. Prior to OSC analysis, the samples were reduced under H_2 at 773 K for 1 h and heated to 1073 K in flowing He. Then, the samples were cooled to 723 K and remained at this temperature during the analysis. The mass spectrometer was used to measure the composition of the reactor effluent as a function time while a 5% O_2/He mixture was passed through the catalyst. Oxygen consumption was calculated from the curve corresponding to $m/e = 32$ taking into account a previous calibration of the equipment.

2.6. Partial oxidation of ethanol

The reaction experiments were performed in a 10 mm ID quartz reactor at atmospheric pressure and 573 K ($W/F = 0.16\ g\ s\ cm^{-3}$). For all of the reactions the catalysts were diluted with a 3:1 ratio of SiC to catalyst to minimize heat effects. Before the reaction, the catalysts were reduced at 773 K for 1 h and then purged under N_2 at the same temperature for 30 min. The reactants were fed to the reactor by bubbling air (30 $cm^3\ min^{-1}$) and N_2 (30 $cm^3\ min^{-1}$) through two saturators containing ethanol at 319 K, in order to obtain the desired ethanol/O_2 ratio (2:1). Although the value of ethanol/O_2 ratio of 0.67 is theoretically the best for hydrogen production, Cavallaro et al. [24] showed that ethanol conversion is around 100% and H_2 production reaches a maximum when using an ethanol/O_2 ratio between 1.7 and 2.5. The exit gases were analyzed using two gas chromatographs equipped with a flame ionization and a thermal conductivity detectors, respectively.

The selectivity to hydrocarbons and oxygenated products (S_x) were calculated from

$$S_x = \frac{y_x}{y_M + y_{acetal} + y_{acid}} \times 100 \quad (1)$$

where y_x is the weight fraction of the methane (x = M), acetaldehyde (x = acetal) or acetic acid (x = acid).

Table 1
BET surface areas for all catalysts

Catalyst	BET surface area ($m^2\ g_{catal}^{-1}$)
Pt/Al_2O_3	180
Pt/ZrO_2	20
Pt/CeO_2	14
$Pt/Ce_{0.50}Zr_{0.50}O_2$	43

3. Results and discussion

3.1. BET surface area

Table 1 shows BET surface areas obtained for all catalysts. Pt/Al_2O_3 catalyst present the highest surface area. The addition of Zr to ceria increased the surface area of the catalysts from 14 to 43 $m^2\ g^{-1}$. Terribile et al. [25] obtained similar values of surface area for Ce–ZrO_2 supports prepared by co-precipitation method. The enhancement of the surface area with the addition of zirconia to ceria was also observed by Hori et al. [23].

3.2. X-ray diffraction (XRD)

The X-ray diffraction patterns of all supports obtained after calcination at 1073 K are presented in Fig. 1. The X-ray diffraction pattern of Al_2O_3 support shows the lines characteristic of γ-alumina. A monoclinic phase (JCPDS – 13-307) for ZrO_2 support and a cubic phase (JCPDS – 4-0593) for CeO_2 were observed.

For $Ce_{0.50}Zr_{0.50}O_2$ support, a shift of ceria peaks from $2\theta = 28.6°$ to $2\theta = 29.3°$ and from $2\theta = 33.1°$ to $2\theta = 33.8°$ was observed. Similar results were obtained by Hori et al. [23] and Fornasiero et al. [26] for $Ce_{0.50}Zr_{0.50}O_2$ support. According to these authors, this shift is related to the formation of a CeO_2–ZrO_2 solid solution with a cubic symmetry.

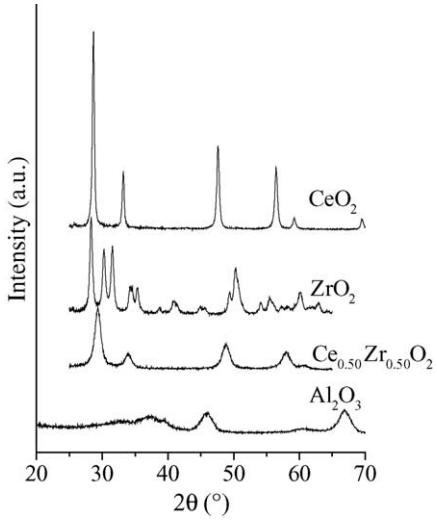

Fig. 1. X-ray diffraction patterns of Al_2O_3, ZrO_2, CeO_2 and $Ce_{0.50}Zr_{0.50}O_2$ supports.

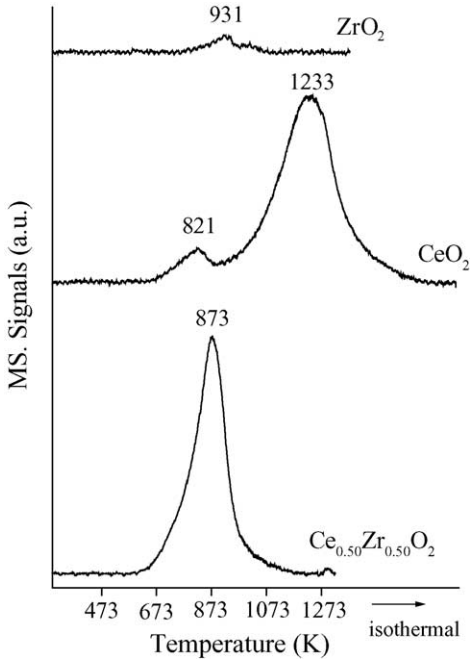

Fig. 2. Temperature-programmed reduction profiles of ZrO_2, CeO_2 and $Ce_{0.50}Zr_{0.50}O_2$ supports.

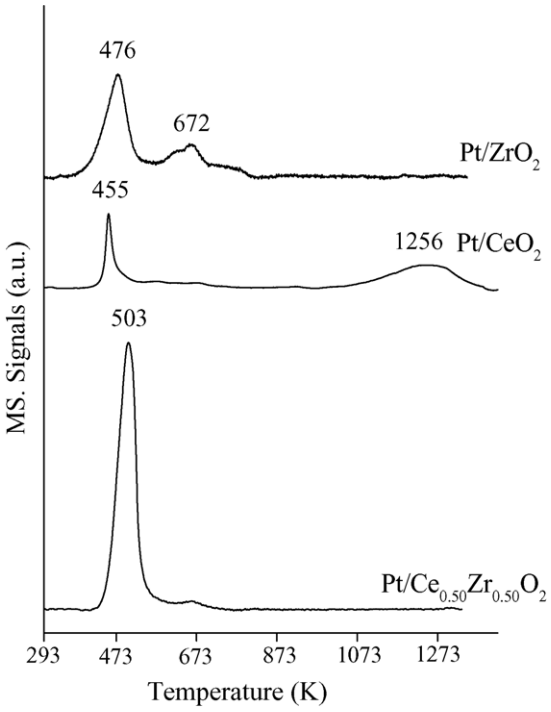

Fig. 3. Temperature-programmed reduction profiles of Pt/ZrO_2, Pt/CeO_2 and $Pt/Ce_{0.50}Zr_{0.50}O_2$ catalysts.

3.3. Temperature-programmed reduction (TPR)

Fig. 2 shows the TPR profiles of ZrO_2, CeO_2 and $Ce_{0.50}Zr_{0.50}O_2$ supports. For ZrO_2 support, only a small H_2 consumption around 931 K was observed, indicating that zirconium oxide was practically irreducible. Bozo et al. [27] obtained similar results in TPR experiments for zirconia.

CeO_2 support presented a small H_2 uptake at 821 K and a strong H_2 consumption at 1233 K. According to the literature [26–31], the first peak is attributed to the surface reduction of CeO_2 and the second one to the formation of Ce_2O_3.

$Ce_{0.50}Zr_{0.50}O_2$ support exhibited a strong H_2 consumption at 873 K. A comparison between the TPR profiles of CeO_2 and $Ce_{0.50}Zr_{0.50}O_2$ supports shows that the addition of 50% of Zr to CeO_2 promotes the reduction of the bulk ceria. Several authors [27,29,32] also observed this promoting effect on the TPR profiles of Ce–ZrO_2 oxides and it was attributed to an improvement of the oxygen mobility induced by the insertion of ZrO_2 into the CeO_2 lattice.

Fig. 3 shows the TPR profiles of the Pt/ZrO_2, Pt/CeO_2 and $Pt/Ce_{0.50}Zr_{0.50}O_2$ catalysts. The Pt/ZrO_2 catalyst showed H_2 uptakes at 476 K and above 573 K. According to stoichiometric calculation, the first peak was assigned to PtO_2 reduction, while the H_2 consumption at temperatures higher than 573 K was attributed to the support reduction. The TPR profile of the Pt/CeO_2 catalyst presented two peaks at 455 and 1256 K. The H_2 consumption at 455 K was higher than the one related to the complete reduction of platinum oxide. This hydrogen uptake corresponds not only to the PtO_2 reduction but also to the surface CeO_2 reduction promoted by the metal. The peak at 1256 K was ascribed to bulk CeO_2 reduction.

$Pt/Ce_{0.50}Zr_{0.50}O_2$ catalyst exhibited a TPR peak at around 503 K that may be attributed to the reduction of both platinum oxide and ceria–zirconia mixed oxide promoted by platinum.

The comparison of the TPR profiles of supports and catalysts revealed that the addition of Pt promoted the reduction of zirconia, ceria and ceria–zirconia support. This promoting effect is due to the hydrogen spillover from metal particles onto the support [28].

3.4. Oxygen storage capacity (OSC)

The oxygen consumption measured for all catalysts are listed in Table 2. Pt/Al_2O_3 catalyst did not present oxygen consumption. The O_2 uptake determined for Pt/ZrO_2 catalyst was very low. On the other hand, the oxygen storage capacity of Pt/CeO_2 and $Pt/Ce_{0.50}Zr_{0.50}O_2$ catalysts were considerably higher than the one of the Pt/ZrO_2 catalyst. Moreover, a comparison between the oxygen consumption obtained for Pt/CeO_2 catalyst and that observed for $Pt/Ce_{0.50}Zr_{0.50}O_2$ catalyst showed that the latter presented the higher oxygen storage capacity. According to the literature [28,33], cerium oxide acts as an oxygen buffer by storing/releasing O_2 due to

Table 2
O_2 uptakes measured at 723 K

Catalyst	O_2 uptake ($\mu mol\ g_{catal}^{-1}$)
Pt/Al_2O_3	0
Pt/ZrO_2	9
Pt/CeO_2	194
$Pt/Ce_{0.50}Zr_{0.50}O_2$	696

the Ce^{4+}/Ce^{3+} redox couple [33]. Because of this redox property, cerium has a high oxygen exchange capacity, which is promoted by the incorporation of ZrO_2 into CeO_2 lattice. The formation of a solid solution increases the oxygen vacancies of the support, increasing its reducibility. This result agrees with the TPR measurements. Then, the higher oxygen storage capacity obtained for $Pt/Ce_{0.50}Zr_{0.50}O_2$ catalyst can be attributed to the high oxygen mobility of the solid solution formed, as identified by XRD data.

3.5. Partial oxidation of ethanol

Fig. 4 shows the ethanol conversion as a function of time on stream (TOS) on partial oxidation of ethanol at 573 K and $W/F = 0.16\ g\ s\ cm^{-3}$. All catalysts presented similar initial conversion and they were quite stable.

Pt/Al_2O_3 catalyst did not present H_2 and CO production. Pt/ZrO_2, Pt/CeO_2 and $Pt/Ce_{0.50}Zr_{0.50}O_2$ catalysts showed approximately the same H_2 yield (0.7–0.8 H_2 mol/consumed ethanol mol) and CO yield (0.5–0.7 CO mol/consumed ethanol mol).

The selectivity to hydrocarbons and oxygenated products (selectivity to HC) obtained at a similar conversion are presented in Fig. 5. On Pt/Al_2O_3 catalyst, the only product was acetic acid. Although several authors reported that ethene is the main product obtained on alumina supports for steam reforming of ethanol at low temperatures [18], its formation was not observed on our Pt/Al_2O_3 catalyst on partial oxidation of ethanol. This fact could be attributed to the presence of oxygen, that favors the production of oxygenated products. For the others catalysts, acetaldehyde as well as methane were observed (Fig. 5). However, the acetaldehyde formation was higher on Pt/ZrO_2 catalyst. These results indicate that the nature of the support plays an important role on the product distribution of the ethanol partial oxidation reaction.

Badlani and Wachs [34] studied the adsorption of methanol on different metal oxides. According to the products obtained on methanol oxidation, the supports were classified as redox, acidic and basic oxides. On the redox oxides, the main products were methyl formiate and formaldehyde. CeO_2 was an example of redox oxide. On the other hand, dimethyl ether and CO_2 were the main products on acidic and basic supports, respectively. Alumina and niobium oxide were examples of acidic support, while yttria represented a basic oxide. Zirconia was a redox/basic metal oxide.

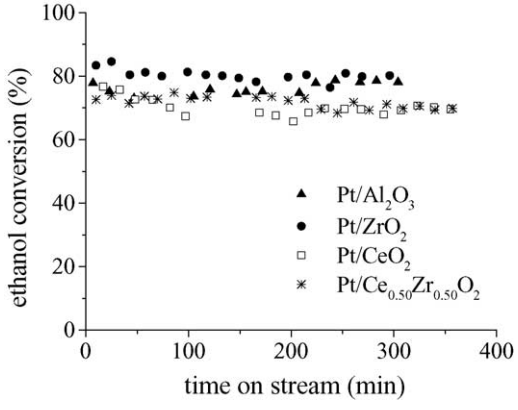

Fig. 4. Ethanol conversion obtained for all catalysts as a function of time on stream (TOS) on partial oxidation of ethanol ($T_{reaction} = 573$ K and $W/F = 0.16\ g\ s\ cm^{-3}$).

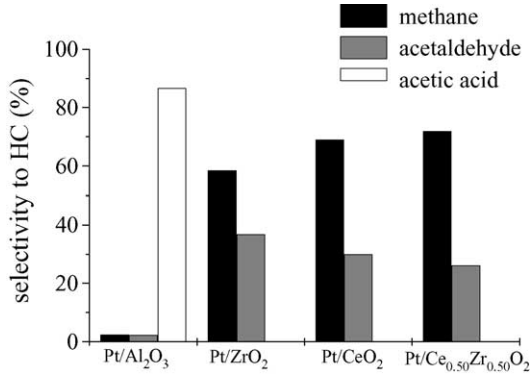

Fig. 5. Selectivity to HC on partial oxidation of ethanol at the same conversion obtained for all catalysts.

Recently, we proposed a reaction mechanism that explained the product distribution on partial oxidation of ethanol over Pt/CeO_2 catalysts based on the IR and TPD experiments [20]. According to this mechanism, adsorption of ethanol on the support give rise to ethoxy species. A fraction of this ethoxy species can be dehydrogenated and further react with oxygen from the support producing acetate species and/or may desorb as acetaldehyde. A higher oxygen storage capacity of the support led to a higher formation of acetate species. At high temperatures, the acetate species can be decomposed to CH_4 and/or oxidized to CO_2 via carbonate species.

In this work, the lower oxygen storage capacity obtained for Pt/ZrO_2 catalyst suggests that the formation of ethoxy species on ZrO_2 support is higher than that obtained for CeO_2 and $Ce_{0.50}Zr_{0.50}O_2$ supports. According to the mechanism described above, the ethoxy species can be dehydrogenated and desorb as acetaldehyde. This effect seems to be more significant on Pt/ZrO_2 catalyst and could explain the higher selectivity to acetaldehyde observed on this catalyst. The redox properties of CeO_2 and $Ce_{0.50}Zr_{0.50}O_2$ supports favored the production of oxidation intermediate products such as acetate species, which could be decomposed to methane. This result agrees very well with the catalytic test. Alumina does not exhibit redox properties, as revealed by our OSC experiments, and then the production of acetic acid could be assigned to its acidic properties.

Taking into account the results obtained, the Pt/CeO_2 and $Pt/Ce_{0.50}Zr_{0.50}O_2$ catalysts revealed to be the best catalysts for fuel processors to PEM fuel cell based on the partial oxidation of ethanol since they exhibited good stability and activity on this reaction. Furthermore, the main by-product detected is methane, which is acceptable in the fuel

cell systems, because methane is combusted as a fuel in the reformer.

4. Conclusions

The results showed that the nature of the support strongly affects the product distribution obtained on partial oxidation of ethanol over supported platinum catalysts. On Pt/Al_2O_3 catalyst, acetic acid was the main product obtained. Its formation was attributed to acidic properties of the alumina support. On Pt/ZrO_2, Pt/CeO_2 and $PtCe_{0.50}Zr_{0.50}O_2$ catalysts, the main products observed were methane and acetaldehyde. Moreover, Pt/ZrO_2 catalyst gave the higher acetaldehyde formation, which could be attributed to its lower oxygen storage capacity, as revealed by the OSC experiments. A lower oxygen exchange capacity will lead to a higher production of ethoxy species, which can be dehydrogenated and desorb as acetaldehyde. On CeO_2 and $Ce_{0.50}Zr_{0.50}O_2$ supports, the higher oxygen exchange capacity favors the formation of acetate species, which will lead to the production of methane and CO_2.

Acknowledgements

The authors wish to acknowledge the financial support of the CNPq and CNPq/Edital Universal program (476954/01-0). The authors also thank Dr. Fabio Barbosa Passos for the TPR experiments.

References

[1] R. Ramachandran, R.K. Menon, Int. J. Hydrogen Energy 23 (1998) 593.
[2] J. Armor, Appl. Catal. A: Gen. 176 (1999) 159.
[3] J. Petrovic, J. Milliken, P. Devlin, C. Read, Proceedings of the 2003 Fuel Cell Seminar, Miami Beach, FL, 2003, p. 988.
[4] J.R. Rostrup-Nielsen, Phys. Chem. Chem. Phys. 3 (2001) 283.
[5] J. Bentley, R. Derby, Ethanol and fuel cells: converging paths of opportunity, Report for the Renewable Fuels Association, 2002.
[6] N. Takezawa, N. Iwasa, Catal. Today 36 (1997) 45.
[7] F.J. Marino, M. Boveri, G. Baronetti, M. Laborde, Int. J. Hydrogen Energy 26 (2001) 665.
[8] S. Freni, N. Mondello, S. Cavallaro, G. Cacciola, V.N. Parmon, V.A. Sobyanin, React. Kinet. Catal. Lett. 71 (2000) 143.
[9] V.V. Galvita, G.L. Semin, V.D. Belyaev, V.A. Semikolenov, P. Tsiakaras, Sobyanin, Appl. Catal. A: Gen. 220 (2001) 123.
[10] A.N. Fatsikostas, D.I. Kondarides, X.E. Verykios, Chem. Commun. 851 (2001).
[11] S. Cavallaro, N. Mondello, S. Freni, J. Power Sources 102 (2001) 198.
[12] V. Klouz, V. Fierro, P. Denton, H. Katz, J.P. Lisse, S. Bouvot-Mauduit, C. Mirodatos, J. Power Sources 105 (2002) 26.
[13] M.A. Goula, S.K. Kontou, P.E. Tsiakaras, Appl. Catal. B: Environ. 49 (2004) 135.
[14] A.N. Fatsikostas, X.E. Verykios, J. Catal. 225 (2004) 439.
[15] J. Comas, F. Mariño, M. Laborde, N. Amadeo, Chem. Eng. J. 98 (2004) 61.
[16] J.P. Breen, R. Burch, H.M. Coleman, Appl. Catal. B: Environ. 39 (2002) 65.
[17] M.S. Batista, R.K.S. Santos, E.M. Assaf, J.M. Assaf, E.A. Ticianelli, J. Power Sources 124 (2003) 99.
[18] J. Llorca, N. Homs, J. Sales, P.R. de la Piscina, J. Catal. 209 (2002) 306.
[19] A.N. Fatsikostas, D.I. Kondarides, X.E. Verykios, Catal. Today 75 (2002) 145.
[20] L.V. Mattos, F.B. Noronha, Appl. Catal. B: Environ., submitted for publication.
[21] P.-Y. Sheng, A. Yee, G.A. Bowmaker, H. Idriss, J. Catal. 208 (2002) 393.
[22] D.K. Liguras, K. Goundani, X.E. Verykios, Int. J. Hydrogen Energy 29 (2004) 419.
[23] C.E. Hori, H. Permana, K.Y. Ng Simon, A. Brenner, K. More, K.M. Rahmoeller, D. Belton, Appl. Catal. B 16 (1998) 105.
[24] S. Cavallaro, V. Chiodo, A. Vita, S. Freni, J. Power Sources (2003) 10.
[25] D. Terribile, A. Trovarelli, J. Llorca, C. de Leitenburg, G. Dolcetti, Catal. Today 43 (1998) 79.
[26] P. Fornasiero, G. Balducci, R. Di Monte, J. Kaspar, V. Sergo, G. Gubitosa, A. Ferrero, M. Graziani, J. Catal. 164 (1996) 173.
[27] C. Bozo, N. Guilhaume, E. Garbowski, M. Primet, Catal. Today 59 (2000) 33.
[28] J. Kaspar, P. Fornasiero, M. Graziani, Catal. Today 50 (1999) 285.
[29] F. Fally, V. Perrichon, H. Vidal, J. Kaspar, G. Blanco, J.M. Pintado, S. Bernal, G. Colon, M. Daturi, J.C. Lavalley, Catal. Today 59 (2000) 373.
[30] C. de Leitenburg, A. Trovarelli, J. Llorca, F. Cavani, G. Bini, Appl. Catal. A 139 (1996) 161.
[31] R.S. Monteiro, F.B. Noronha, L.C. Dieguez, M. Schmal, Appl. Catal. A 131 (1995) 89.
[32] H. Vidal, J. Kaspar, M. Pijolat, G. Colon, S. Bernal, A. Cordón, V. Perrichon, F. Fally, Appl. Catal. B 27 (2000) 49.
[33] M.H. Yao, R.J. Baird, F.W. Kunz, T.E. Hoost, J. Catal. 166 (1997) 67.
[34] M. Badlani, I. Wachs, Catal. Lett. 75 (2001) 137.